New Journal and we have not received input yet 34 (2022) 101402

Contents lists available at ScienceDirect

Thermal Science and Engineering Progress

journal homepage: www.sciencedirect.com/journal/thermal-science-and-engineering-progress

Ultrasonic technique for measuring the mean flow velocity behind a throttle: A metrological analysis

Sameh Alsaqoor [a], Ali Alahmer [a,b], Artur Andruszkiewicz [c], Piotr Piechota [c], Piotr Synowiec [c], Nabil Beithu [a,d], Wiesław Wędrychowicz [c], Elżbieta Wróblewska [c], Hussam Jouhara [e,f,*]

[a] Department of Mechanical Engineering, Faculty of Engineering, Tafila Technical University, P. O. Box 179, 66110 Tafila, Jordan
[b] Department of Industrial and Systems Engineering, Auburn University, Auburn, AL 36849, United States
[c] Wrocław University of Science and Technology, Faculty of Mechanical and Power Engineering, Department of Thermal Sciences, Wybrzeże Stanisława Wyspiańskiego 27, 50-370 Wrocław, Poland
[d] Department of Mechanical and Industrial Engineering, Applied Science Private University, P.O. Box 166, 11931 Amman, Jordan
[e] Heat Pipe and Thermal Management Research Group, College of Engineering, Design and Physical Sciences, Brunel University London, UB8 3PH, UK
[f] Vytautas Magnus University, Studentu Str. 11, LT-53362 Akademija, Kaunas Distr., Lithuania

ARTICLE INFO

Keywords:
Ultrasonic flowmeter
Turbulent flow
Measurement error
Throttle (butterfly valve)
Accuracy

ABSTRACT

This article discusses an ultrasonic technique for monitoring liquid flow. The mean velocity of the flow behind an obstruction in the throttle type was measured using an ultrasonic flow meter. Furthermore, the equations used to analyze the velocity distribution in a distorted turbulent flow are presented. The measurement findings were compared with those of separate velocity distribution models to select the best equation for characterizing the measured flow. Measurements were taken for two distinct throttle settings by varying the distance from the throttle and angle of the flowmeter head position. The measurements were performed to determine the order of measurement errors if the ultrasonic flowmeter was installed behind the obstruction, without retaining the appropriate distances. The results of, experiments conducted behind a throttle allowed us to conclude that the distance between the measurement location and the barrier affected the accuracy of the acquired results.

Introduction

It is necessary to know or measure the mean velocity of a fluid flow to address thermal flow issues. The flow rate (mass or volume) is determined by measuring the mean velocity, which is a critical component of balancing devices and systems [1]. Therefore, it is essential to develop a highly accurate method for the measuring fluid flow velocities [2,3]. Another desirable quality of the measuring device for the mean flow velocity is its non-invasive and non-contact capability. In this situation, the assembly and functioning of the measuring device do not cause the installation to stop or affect the flow. Ultrasonic velocity measurement is widely utilized in flow practice owing to its high measurement accuracy [4]. This method is non-contact and non-invasive, as it does not interfere with the geometry or functionality of the installation. Ultrasonic flow meters are available in various designs and can be divided into two categories based on the signal processing methods: Doppler shift and transit time flow meters. The two-phase flows were measured using an ultrasonic velocity method based on the Doppler effect. This necessitates the presence of solid particles or air bubbles in the tested liquids, which can reflect the signal.

Much research has been conducted to visualize flow profiles and measure the mean velocities of fluid flows. Renaldas et al. [5] demonstrated that recesses alter the symmetry of flow profiles along the ultrasonic pathways. Calculating the total flow rate without considering the local nature of the profile might result in a measurement error. According to Rajita et al. [6], multipath ultrasonic instruments can produce more accurate flow rates that are more accurate than those produced by single-path ultrasonic instruments. Tang [7] developed a multichannel ultrasonic gas flow meter to increase the measurement precision by enlarging the ultra-sound paths or modifying their layout to prolong the ultrasonic propagation route. Sun et al. [8] presented a new hybrid approach, combined computational fluid dynamics (CFD), wave acoustics, and ray acoustics. High-precision readings are more difficult to obtain using small-diameter ultrasonic flow meters. Chen et al. [9] proposed a dual-channel ultrasonic gas flow meter configuration, and

* Corresponding author at: Heat Pipe and Thermal Management Research Group, College of Engineering, Design and Physical Sciences, Brunel University London, UB8 3PH, UK.
E-mail address: Hussam.Jouhara@brunel.ac.uk (H. Jouhara).

https://doi.org/10.1016/j.tsep.2022.101402
Received 1 May 2022; Received in revised form 25 June 2022; Accepted 1 July 2022
Available online 4 July 2022

Nomenclature

a, n, k, m	velocity distribution equations coefficients
c	ultrasonic wave transit velocity, m/s
CFD	computation fluid dynamics
D	diameter of the pipeline, mm
DN	distance measured in multiples of the nominal diameter of the pipeline
K	correction factor for measurement data (v_{thr}, v_p), –
$K_{t,i}$	correction factor for the velocity distribution models $(i = 1, \cdots, 14)$, –
M_i	theoretical model of distorted velocity distribution $(i = 1, \cdots, 14)$, –
r	coordinate of the location for the velocity plane, mm
R	pipeline radius, mm
Re	Reynolds number
S	cross-sectional area, m^2
t1	time for the ultrasonic wave to travel downstream, s
t2	time for the ultrasonic wave to travel upstream, s
$v_i\,(r, \theta)$	equation of the velocity distribution of the distorted turbulent flow $(i = 1, \cdots, 14)$, m/s
v_a	flow velocity along the main axis of the pipeline,m / s
v_c	average velocity of the liquid flow along the path of the ultrasonic wave, m/s
v_d	average velocity of liquid flow in the cross-section of the pipeline, m/s
v_p	flow velocity measured on a straight section of the pipeline (reference), m/s
v_{thr}	flow velocity measured behind the throttle,m / s
α	setting angle of ultrasonic heads,°
Δt	difference of the ultrasonic wave transit times "downstream" and "upstream" of the flow, s
sδdev	maximum device error, m/s
δinst	maximum assembly error, m/s
δmes	limit error, m/s
θ	angular coordinate for the velocity distribution

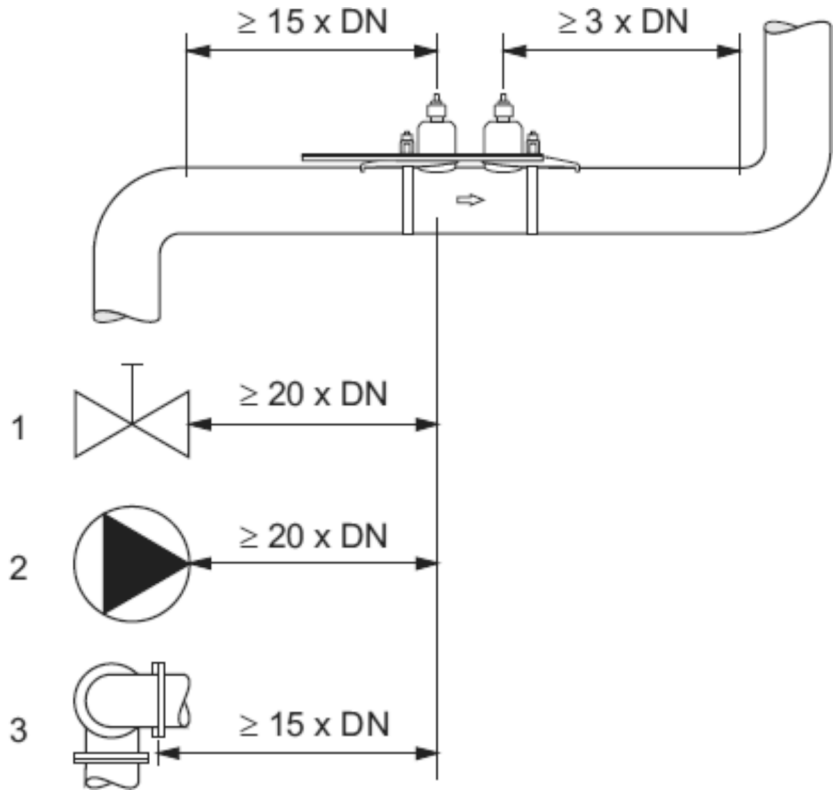

Fig. 1. Recommended straight sections when installing ultrasonic heads behind obstacles.

evaluated its measured properties under various pipe installation situations. Qin et al. [10] suggested an intelligent approach to flow profile recognition for multipath ultrasonic flowmeters relying on support vector machines to improve measurement accuracy. Palau et al. [11] introduced a numerical analysis using CFD to examine pipeline water flow patterns and quantify monitoring errors introduced by different valves in pressurized pipe networks. Different settings of the gate and butterfly valves mounted on 3DN, and 6DN m from the flowmeters were numerically simulated. The results revealed that the placement of a butterfly valve 3DN or 6DN away from the electromagnetic meter provided greater measurement accuracy, according to the ISO 4064 standard. Zhang et al. [12] studied the influence of the velocity profiles throughout a pipe on the propagation time of ultrasonic waves. To enhance measurement accuracy, the authors proposed a theoretical adjustment for transit-time ultrasonic flowmeters for both laminar and turbulent flows. Mahadeva et al. [13] improved the measurement precision by varying the spacing between transducers. Awad et al. [14] estimated the mean liquid flow velocity and uncertainty by using analytical and Monte Carlo simulation approaches.

Maintaining the straight pipeline sections required by standards in front of and behind an obstruction may be a considerable challenge when using the ultrasonic approach. This is particularly common for

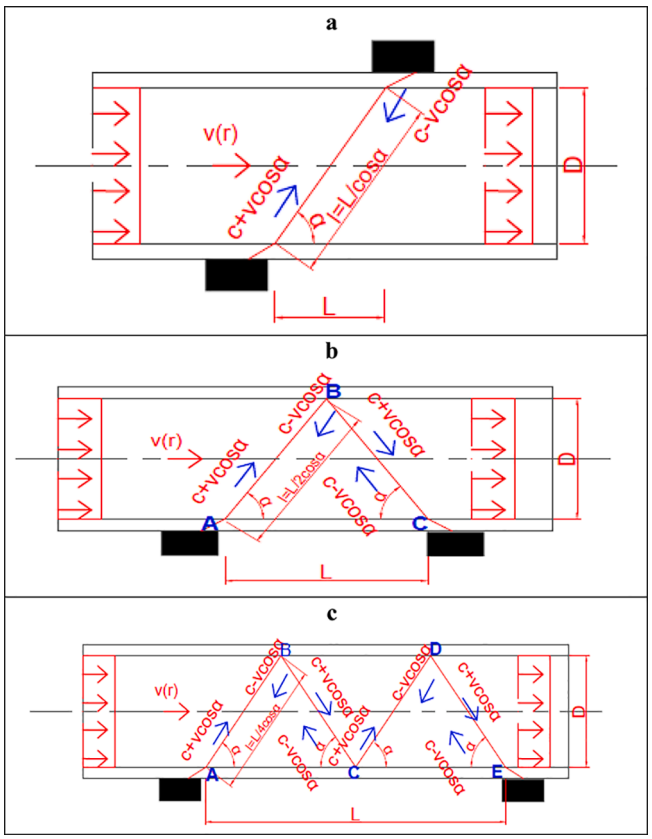

Fig. 2. Changes in the angles of the ultrasonic flowmeter heads (Fig. 2a setting of "Z" type; Fig. 2b setting of "V" type; Fig. 2c setting of "W" type).

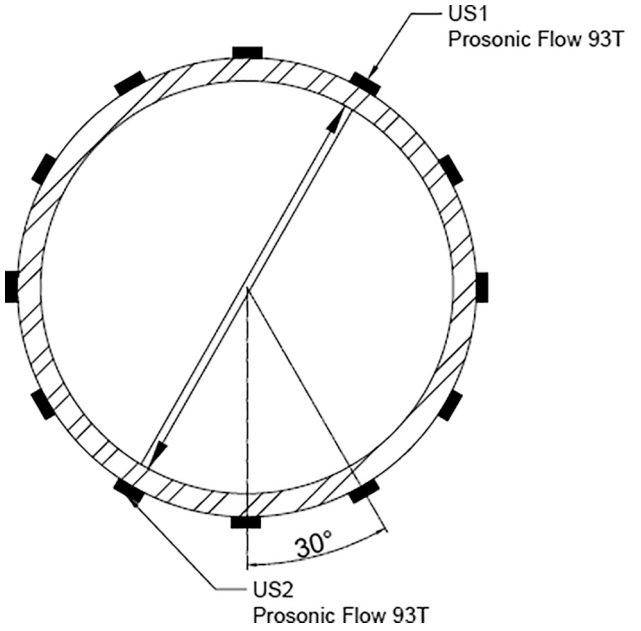

Fig. 3. Changes in the angle of the ultrasonic flowmeter heads (every 30°).

pipes with diameters greater than 1 m. The required straight sections are generally 15DN–20DN, depending on the obstacle, as shown in Fig. 1.

In industrial or power energy installations with large diameters, it is difficult to find straight sections of pipeline 15DN-20DN in length. Consequently, it is recommended to conduct research that allows for the investigation of the influence of obstructions (knees, gate valves, constrictions, and throttles) on ultrasonic flow-meter readings. Previous studies [15–17] have addressed the issue of ultrasonic flow measurement under non-standard measurement settings downstream of a pipeline elbow. This study focused on the data acquired downstream of a butterfly valve with a manual closing angle.

The transit time method of measurement

The transit-time technique is designed for single-phase flows, and the difference in transit times of the ultrasonic waves in the flow direction ("downstream") and in the opposite direction ("upstream") is the physical foundation for the functioning of this type of flowmeter.

Eqs. (1) and (2) describe the period of passage of the ultrasonic wave "downstream" and "upstream" of the flow, respectively. Eq. (3) is obtained by transforming Eqs. (1) and (2), respectively. The flow velocity for the fundamental method of adjusting the heads of the z-type flowmeter, as shown in Fig. 2 (a), is given by Eq. (3).

$$t_1 = \frac{l}{c + v \bullet sin\alpha} + \sum_{i=1}^{n} \frac{l_1}{c_1} \tag{1}$$

$$t_2 = \frac{l}{c - v \bullet sin\alpha} + \sum_{i=1}^{n} \frac{l_1}{c_1} \tag{2}$$

$$\Delta t = \frac{2 \bullet l \bullet sin\alpha}{(v \bullet sin\alpha - c) \bullet (v \bullet sin\alpha + c)} \tag{3}$$

The heads can be arranged in various ways and placed on the pipeline in different ways, as depicted in Fig. 2:

- "Z" – A single-route ultrasonic wave appropriate for use in large diameter pipes.
- "V" – dual route of the ultrasonic wave; an extended path of the ultrasonic wave is employed to improve measurement accuracy in small-diameter pipelines.
- "W" – quadruple route of the ultrasonic wave; the prolonged path of the ultrasonic wave is used to increase measurement accuracy in small-diameter pipelines.

The aforementioned settings can be used interchangeably depending on the simplicity of their installation. In terms of metrological quality, the methods of situating the heads mentioned above differ from one another. As displayed in Fig. 2a, the Z-type configuration ensured a greater ultrasonic signal value, which affected the accuracy of flow measurement. The V-type setting, as depicted in Fig. 2 (b), is distinguished by the longer path of the ultrasonic wave, which ensures increased measurement precision. The "W" setting, as presented in Fig. 2 (c), provides the wave's longest route. It is important to remember that when the distance between sensors is greater, the signal value needs to be sufficiently high.

Metrological properties of ultrasonic flow meters

The tests were performed using a transit time flow meter with heads installed on the pipeline in a V-type configuration. Ultrasonic flow meters with heads on the pipeline enable non-invasive, high-accuracy flow measurements. According to manufacturers, ultrasonic flow meters are reported to be accurate to within 2%. Only multipath flow meters can achieve a device accuracy of less than 1% of the observed value. To achieve the claimed measurement accuracy, straight parts of the pipeline must be preserved upstream and downstream of any obstruction that disturbs the flow, as indicated in the manufacturer's guidelines and recommendations. Hydraulic elbows and bends, throttles, gate valves, other valves, and reducers are typical fittings that can disrupt the flow and significantly impact the measurement results.

The maximum measurement error for a measuring point of the

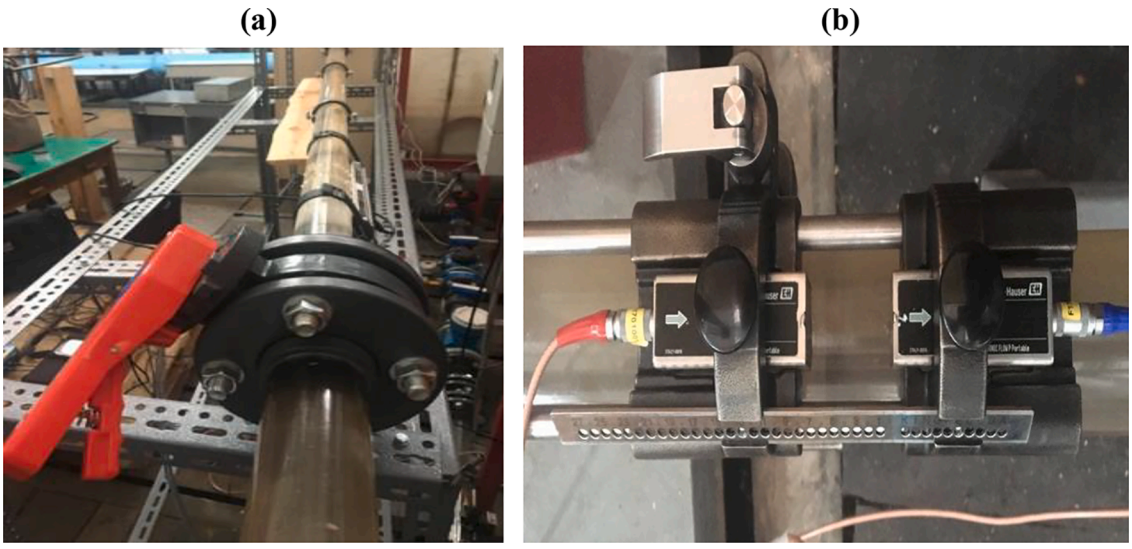

Fig. 4. (a) Throttle (butterfly valve); (b) Installation of ultrasonic flowmeter heads – V-type setting.

Table 1
Summary of measurement data for the 1DN,5DN,7DN, and 11DN measuring diameter.

1DN													
Throttle opening angle; °	The angle of the heads α; °	0	30	60	90	120	150	180	210	240	270	300	330
75	v_p; m/s	1.649	1.683	1.682	1.674	1.673	1.679	1.688	1.685	1.675	1.674	1.672	1.683
	v_{thr}; m/s	1.474	1.796	1.792	1.593	1.584	1.535	1.677	1.535	1.85	1.794	1.656	1.604
	K; -	1.12	0.94	0.94	1.05	1.06	1.09	1.01	1.10	0.91	0.93	1.01	1.05
90	v_p; m/s	1.708	1.701	1.692	1.688	1.686	1.684	1.693	1.7	1.684	1.678	1.683	1.694
	v_{thr}; m/s	1.528	1.826	1.854	1.641	1.473	1.475	1.643	1.91	1.824	1.549	1.462	1.513
	K; -	1.12	0.93	0.91	1.03	1.14	1.14	1.03	0.89	0.92	1.08	1.15	1.12
5DN													
75	v_p; m/s	1.664	1.662	1.678	1.684	1.669	1.658	1.666	1.667	1.671	1.668	1.676	1.651
	v_{thr}; m/s	1.587	1.586	1.6	1.611	1.619	1.581	1.568	1.59	1.61	1.624	1.639	1.625
	K; -	1.05	1.05	1.05	1.05	1.03	1.05	1.06	1.05	1.04	1.03	1.02	1.02
90	v_p; m/s	1.69	1.69	1.681	1.686	1.695	1.701	1.706	1.709	1.699	1.688	1.691	1.696
	v_{thr}; m/s	1.664	1.662	1.678	1.684	1.669	1.658	1.666	1.667	1.671	1.668	1.676	1.651
	K; -	1.02	1.02	1.00	1.00	1.02	1.03	1.02	1.03	1.02	1.01	1.01	1.03
7DN													
75	v_p; m/s	1.664	1.662	1.678	1.684	1.669	1.658	1.666	1.667	1.671	1.668	1.676	1.651
	v_{thr}; m/s	1.436	1.455	1.496	1.641	1.644	1.669	1.66	1.673	1.66	1.66	1.669	1.669
	K; -	1.16	1.14	1.12	1.03	1.02	0.99	1.00	1.00	1.01	1.00	1.00	0.99
90	v_p; m/s	1.658	1.687	1.685	1.698	1.709	1.699	1.698	1.698	1.694	1.684	1.691	1.687
	v_{thr}; m/s	1.606	1.606	1.598	1.606	1.614	1.567	1.598	1.606	1.606	1.676	1.622	1.598
	K; -	1.03	1.05	1.05	1.06	1.06	1.08	1.06	1.06	1.05	1.00	1.04	1.06
11DN													
75	v_p; m/s	1.669	1.664	1.66	1.652	1.653	1.661	1.674	1.671	1.673	1.669	1.663	1.67
	v_{thr}; m/s	1.583	1.56	1.591	1.583	1.576	1.591	1.576	1.583	1.583	1.583	1.583	1.583
	K; -	1.05	1.07	1.04	1.04	1.05	1.04	1.06	1.06	1.06	1.05	1.05	1.05
90	v_p; m/s	1.705	1.696	1.692	1.705	1.709	1.688	1.684	1.689	1.688	1.693	1.704	1.7
	v_{thr}; m/s	1.669	1.664	1.66	1.652	1.653	1.661	1.674	1.671	1.673	1.669	1.663	1.67
	K; -	1.02	1.02	1.02	1.03	1.03	1.02	1.01	1.01	1.01	1.01	1.02	1.02

Endress + Hauser Prosonic Flow 92 and 93 T ultrasonic flow meters was described in [16]. It can be evaluated as the sum of the measuring device error (δ_{dev}), and ultrasonic head installation error (δ_{inst}). Eq. (4) gives the maximum measurement error at any point in the measurement range, or the error limit:

$$\delta_{mes} = \delta_{dev} + \delta_{inst} = 0.5\% \bullet v_{mes} \pm 7.5\frac{mm}{s} + 1,5\% \bullet v_{mes} = 2\% \bullet v_{mes} + 7.5\frac{mm}{s} \quad (4)$$

Methodology of the measurement process

In this study, we considered turbulent flow with a disturbed velocity distribution. The existence of a throttle with a manual opening angle setting during the installation resulted in a flow disruption. Upstream and downstream of the throttle, measurements were taken using Endress + Hauser Prosonic Flow 93 T and Endress + Hauser Prosonic Flow 92 ultrasonic flow meters that were of the same type and as accurate as each other.

Measurements were taken at different cross-sections behind the

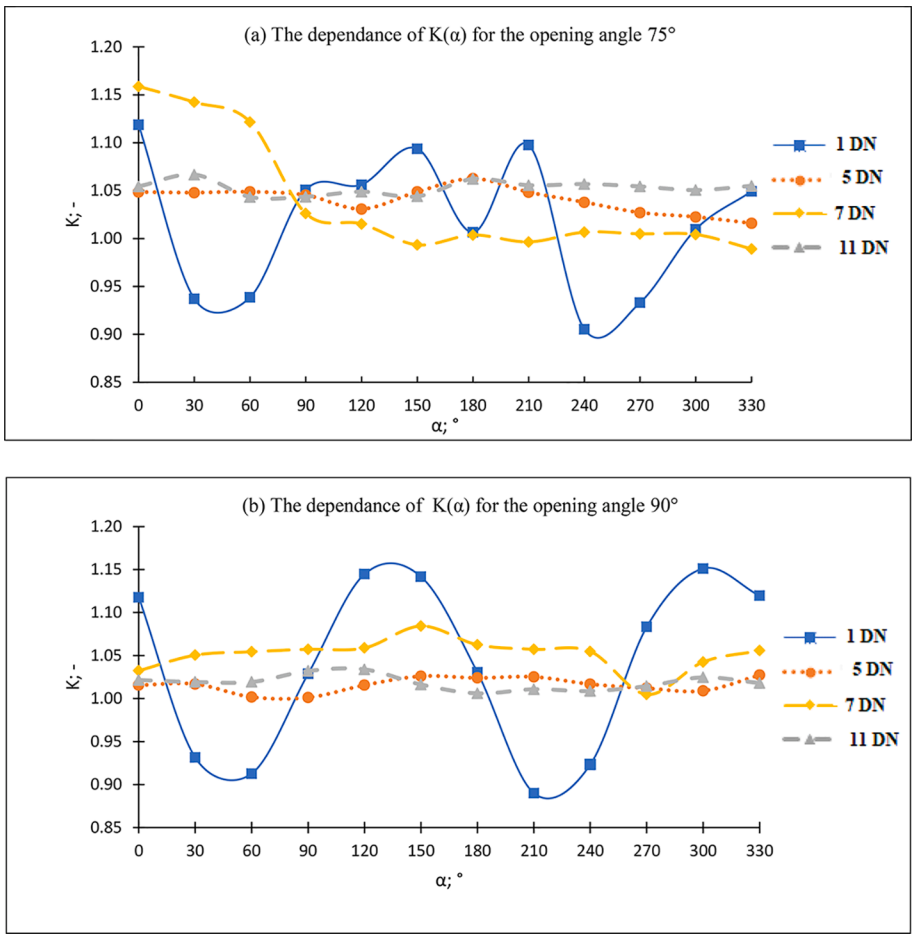

Fig. 5. Variation of K value for various angles of ultrasonic heads at the (a) 75° throttle setting angle; and (b) 90° throttle setting angle.

throttle with an axial separation of the transducers of one diameter (D = 60 mm). A series of tests was carried out to determine the distance at which a flow measurement could be made with an accuracy similar to that provided by the flow meter manufacturer. Therefore, a series of measurements were performed for 12 different ultrasonic head angles for each measurement location. The angular range of 0-330° was investigated by spinning the ultrasonic heads in increments of 30, as shown in Fig. 3.

One measurement series was recorded for ten minutes, with an average time of one second. The recorded data were subjected to metrological analysis after the measurements were conducted to exclude erroneous values that did not fall within the extent of the measurement uncertainty. The remaining data are averaged. Two distinct throttle opening angles were tested: 75° and 90°.

The flow of liquid (water) was monitored experimentally using an ultrasonic technique behind the throttle of the butterfly valve, as depicted in Fig. 4a, at a variable distance from the throttle, that was smaller than the standards indicated. An Endress Hauser Proline Prosonic Flow 93 T ultrasonic flow meter was used to measure the flow velocity behind throttle v_{thr}, as demonstrated in Fig. 4b. The measurement of the flow velocity v_p in the straight section of the pipeline in front of the throttle, while maintaining an appropriate distance from the obstacle, served as the reference value. An Endress Hauser Prosonic Flow 92 ultrasonic flow meter was used as a reference instrument.

Results and analysis

The measurement results for four selected measuring diameters (1DN, 5DN, 7DN, and 11DN) are shown in Table 1. For each of these diameters, measurements were taken for two throttle opening angles (75° and 90°) at 12 different angular separations of the ultrasonic heads. According to Table 1, in the consecutive measurement series (for successive measurement locations and two distinct angles of throttle adjustment), the reference velocity vp varies slightly. This is because of the challenge of maintaining the volume flow constant and remaining unchanged. However, the changes in v_p, though, are insignificant. The dimensionless correction factor K, defined by the velocity ratio v_{thr}/v_p, was adopted as the comparison criterion for the results of the different measurement series. One method of compensating for measurement errors caused by a distorted velocity distribution is to apply a correction factor ($K = \frac{v_p}{v_{thr}}$) to the measurement data. The K coefficient varies based on the angle of the head α, as depicted in Fig. 5.

The relative velocity measurement error for the throttle set at a 75° angle reaches about 12 % in the measuring section at 1DN, and its value significantly changes depending on the angle of the ultrasonic heads. However, the 1DN section has the angles = 180° and = 300°, for which the difference in indicators upstream and downstream of the throttle is less than 1%.

The error values in the measuring cross-section were less than 7% over the whole range and were far less sensitive to the angle of the heads. Apart from the angles of 0°, 30°, and 60°, for which the error values exceed 10% in the measurement cross-section, the error values for the other angles do not exceed 3%. To include a consistent correction factor regardless of the angle of the ultrasonic head setup, the error values for the measuring cross-section at 11DN fell within a restricted range of 4 5 to 6.55.

The flow structure is less disturbed when the throttle is set at a 90° angle than when it is set at a 75° angle. The closest measurement cross-

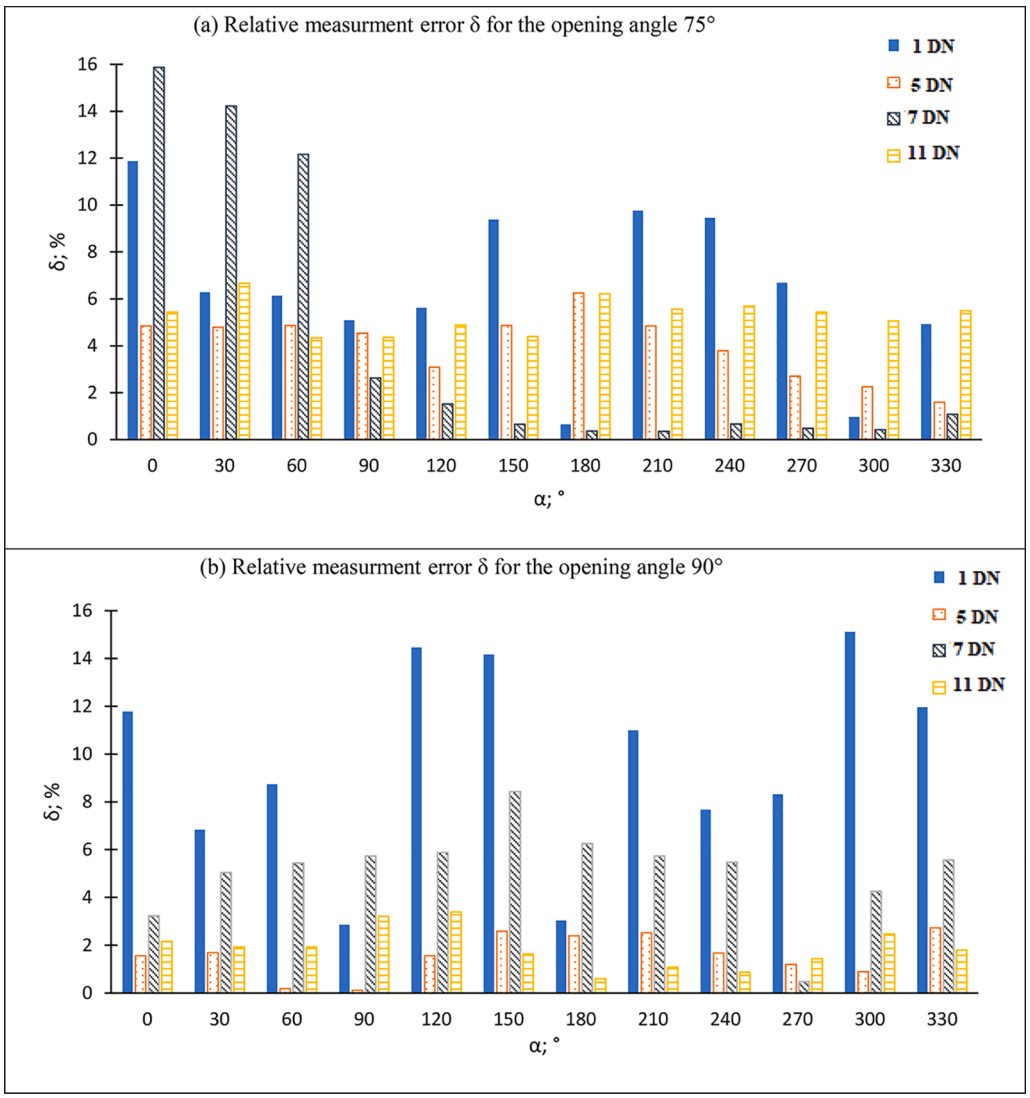

Fig. 6. The dependence of the relative velocity measurement error on the angle of the ultrasonic heads α at the (a) 75° throttle setting; and (b) 90° throttle setting.

Table 2
Parameters of velocity distribution models described by Eq. (5).

Model M_i	N	k	m	a	f(θ)
M1	9	4	$-\frac{0,5}{\pi}$	–	$\theta \bullet \sin\theta$
M2	7	9	$-\frac{0,4}{\pi}$	–	$\theta \bullet \sin\theta$
M3	9	4	$\frac{0,04}{\pi}$	–	$(\theta^2-1) \bullet (1-\cos\theta)^2$
M4	9	0,5	3,1370	0,5	$e^{-a\theta} \bullet \sin\theta$
M5	7	9	$\frac{e^{0,1\pi}}{2}$	0,2	$e^{-a\theta} \bullet \sin\theta$
M6	7	9	$-\frac{e^{0,1\pi}}{2}$	0,2	$e^{-a\theta} \bullet \sin\theta$
M7	9	4	$\frac{2}{\pi^5}$	–	$\theta^2 \bullet (2\pi-\theta)^2$
M8	9	4	$\frac{1}{\pi^2}$	–	$\theta \bullet (1-\cos^2\theta)$
M9	9	4	$\frac{2}{\pi^3}$	–	$\theta \bullet (2\pi-\theta) \bullet \sin^2\theta$
M10	9	9	0,6813	0,1	$e^{-a\theta} \bullet \sin^2\theta$
M11	7	9	$e^{0,1\pi}$	0,2	$e^{-a\theta} \bullet \sin^2\theta$
M12	9	0,5	−6,7501	0,5	$e^{-a\theta} \bullet \sin^2\theta$
M13	7	9	$\frac{1}{2\pi^2}$	–	$(2\pi-\theta)^2 \bullet \theta \bullet sin3\theta$
M14	4	9	$\frac{e^{0,15\pi}}{2}$	0,3	$e^{-a\theta} \bullet sin^2 5\theta$

section to the disturbance's source, 1DN, had the most significant error values. For as many as six different head position angles, the error value δ for this measurement cross-section exceeded 10%. As shown in the diagrams, the following cross-sections (5DN, 7DN, and 11DN) significantly stabilize the flow. Sections 5DN and 11DN had error values of less than 3% and 3.5%, respectively. At cross-section 7DN, the values exhibited notable oscillations, with values in the range of 3–8%.

The values of the relative velocity measurement error $\delta = \frac{|v_p - v_{thr}|}{v_{thr}}$ were calculated using the measurement data in Table 1. These values are graphically shown in Fig. 6.

Adjusting the velocity distribution equations

Review of distorted velocity distribution models

The main issue of this study is turbulent flow with a velocity distribution distorted by the throttle. Studies of velocity distribution models distorted by various types of disturbances have been reported in the literature on fluid mechanics [18–21]. From the obtained equations, fourteen were selected. These equations are an extension of the equations describing the turbulent pipe flow $v_t = v_a \bullet \left[\left(1-\frac{r}{R}\right)^{\frac{1}{n}}\right.$ by the term describing the influence of the disturbance distorting the flow. Table 2 presents the equations considered, v (r, θ).

Table 3
Summary of the calculated values of the Kt coefficient for the M1-M14 velocity distribution models.

Model	1	2	3	4	5	6	7	8	9	10	11	12	13	14
θ;°	Kt													
0	1,025	1,013	0,952	0,977	0,980	0,886	0,988	0,964	1,058	1,101	1,175	0,886	0,940	1,012
30	0,977	0,966	1,012	0,934	0,947	0,919	0,984	0,964	1,018	1,033	1,054	0,980	1,040	0,952
60	0,944	0,934	1,000	0,920	0,929	0,938	0,977	0,999	0,931	0,926	0,896	1,015	0,940	0,871
90	0,933	0,923	0,995	0,926	0,928	0,940	0,975	1,025	0,890	0,889	0,855	0,999	1,319	0,854
120	0,944	0,934	1,000	0,942	0,939	0,927	0,977	0,988	0,931	0,941	0,938	0,959	0,940	0,905
150	0,977	0,966	1,012	0,962	0,958	0,907	0,984	0,910	1,018	1,045	1,092	0,917	0,665	0,979
Type	1 Peak							2 Peak				More		

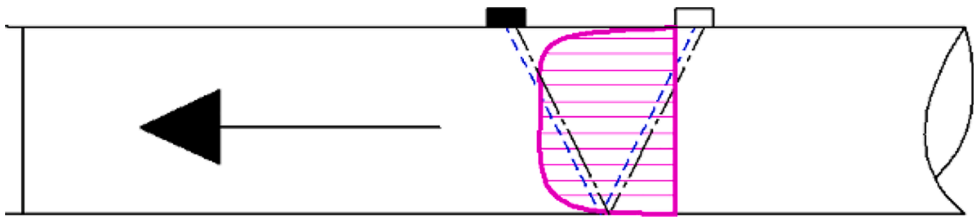

Fig. 7. Assuming unchanging velocity profile between sensors in setting "V".

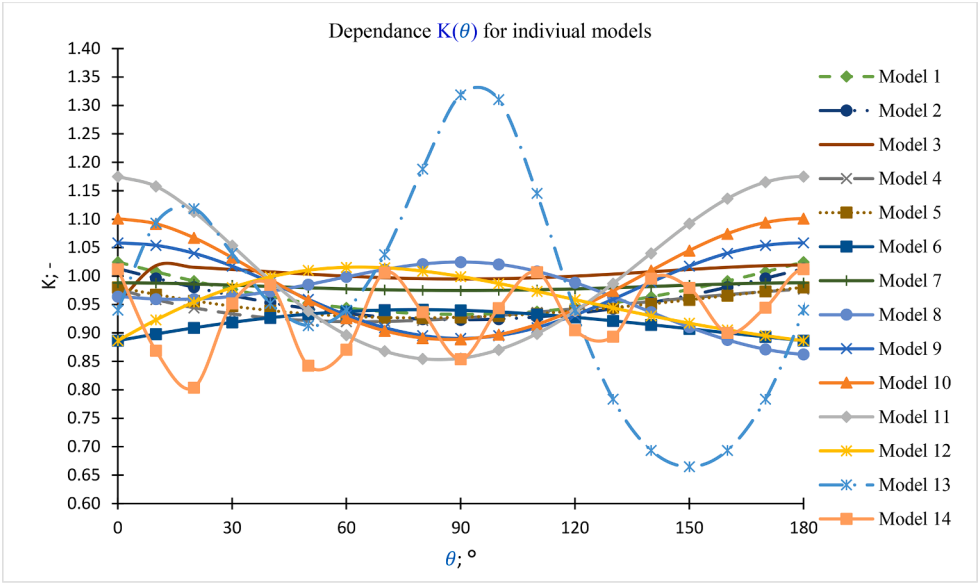

Fig. 8. Variation of Kt value depending on the angle θ for different models of velocity distributions M1-M14.

The general form of the distorted velocity distribution models can be represented by Eq. (5).

$$v_{t\_i}(r,\theta) = v_a \bullet \left[\left(1-\frac{r}{R}\right)^{\frac{1}{n}} + m \bullet \frac{r}{R} \bullet \left(1-\frac{r}{R}\right)^{\frac{1}{k}} \bullet f(\theta)\right] \quad (5)$$

where v_a is the mean velocity along the main axis of the pipeline, n is the coefficient related to the flow number (Reynolds number) Re, and m, k, and a are the coefficients characterizing the distortion of the velocity distribution.

Determination of the K coefficient for models of the distorted velocity distribution

The shape coefficient of the velocity distribution (K_{t_i}, Eq. (6)) was determined using the equations in Table 2, analogous to the correction coefficient K obtained from the measurement data [22,23]. This coefficient is defined as the ratio of the average liquid flow velocity in the pipeline cross-section (v_d, Eq. (7)) to the average liquid flow velocity along the path of the ultrasonic wave (v_c, Eq. (8)) [20]:

$$K_t = \frac{v_d}{v_c} \quad (6)$$

$$v_d = \frac{1}{S}\iint v_t dS \quad (7)$$

$$v_c = \frac{1}{R} \bullet \int_0^R v_t(r)dr \quad (8)$$

The K_t coefficient for Model 1 is derived as follows in Eq. (9) as an example

$$K_{t1} = \frac{v_{d1}}{v_{c1}} = \frac{\frac{1}{S}\iint v_t dS}{\frac{1}{R} \bullet \int_0^R v_t(r)dr} = \frac{\frac{2n^2}{(n+1)\bullet(2n+1)} - \frac{4k^3 \bullet m}{(k+1)\bullet(2k+1)\bullet(3k+1)}}{\frac{n}{n+1} - \frac{\pi \bullet k^2 \bullet m \bullet \sin\theta}{2\bullet(k+1)\bullet(2k+1)}} \quad (9)$$

The derived K_{t_i} coefficients for the distinct models of M1-M14 velocity distributions are listed in Table 3. These coefficients were compared with the K values obtained from the ultrasonic V-head

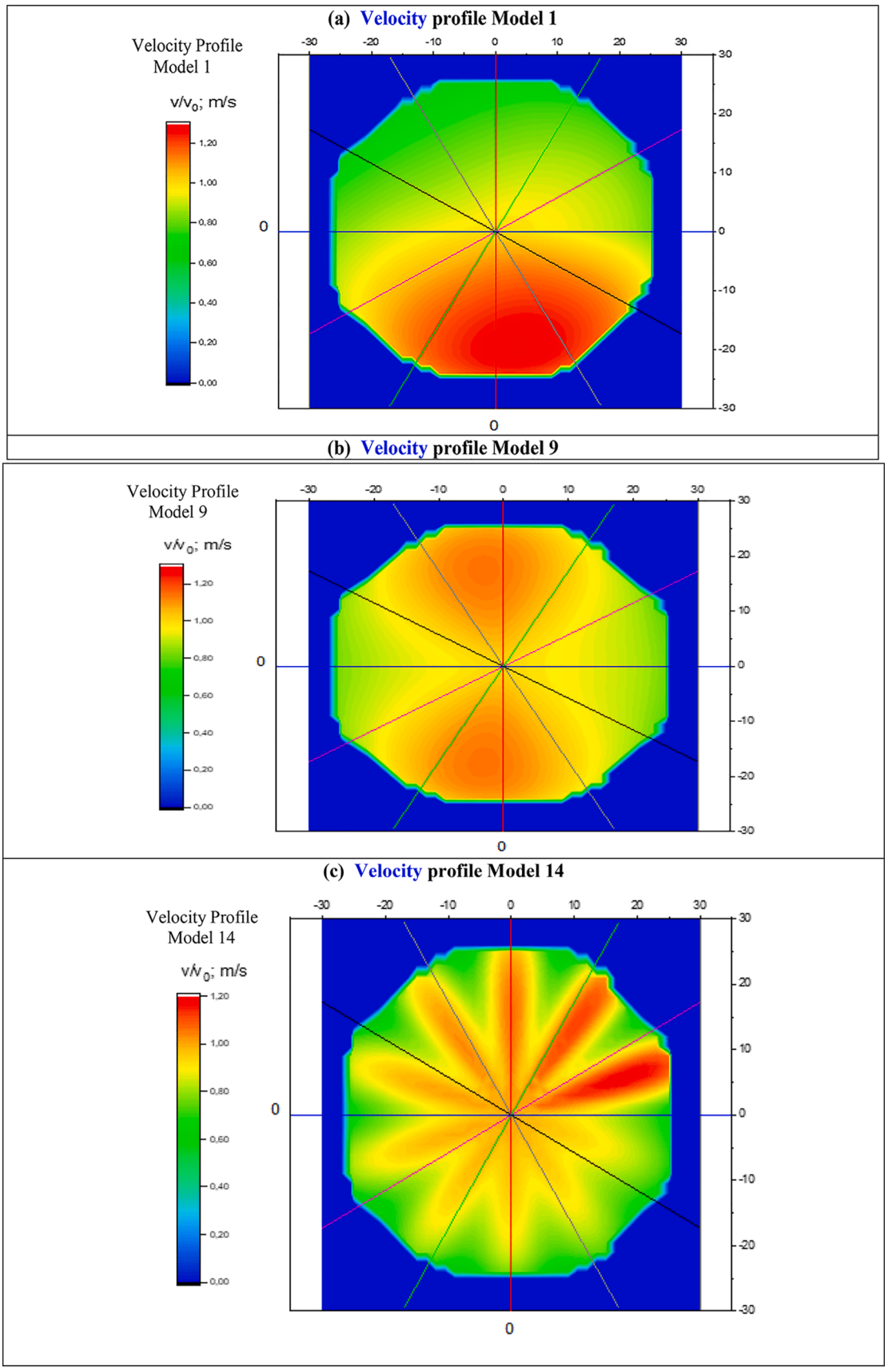

Fig. 9. Velocity profile of the distorted velocity distribution for (a) model 1; (b) model 9; and (c) model 14.

measurements. The following assumptions were made in this study:

1. Over the distance between the transducers, as depicted in Fig. 7, the velocity distribution is invariable and is characterized by the velocity model equation $M_i = 1.0.14$.
2. It was assumed that the emitted and reflected waves were characterized by equations for pairs of data at 0°-180°, 30°-210°,…, 330°–150° as part of the reconstruction of the ultrasonic wave path in the V-head system.

Selection of the optimal velocity distribution model

The examined velocity distribution equations explain various distortions in the velocity distributions in a turbulent flow. The values of the velocity distribution shape coefficient Kt were determined. These values may be related to the K-coefficient values derived from flow velocity measurements. The curves of dependency $K_t(\theta)$ for the measurement data presented in Fig. 5 can be compared with the curves of the same dependence for the velocity distribution models described in Fig. 8. The maximum velocity was evaluated using graphs of the measurement data. Based on the similarity of curve of the dependency $K_t(\theta)$, we selected a velocity distribution model that accurately describes the actual flow for a particular distance from the throttle. The velocity profiles for the selected models from each group are listed below (Model 1, one maximum; Model 9, two maxima; Model 14, three or more maxima), as presented in Fig. 9. The velocity profiles developed in the origin allow us to better comprehend the velocity distribution models under consideration.

Conclusion

Ultrasonic flow measurement is gaining prominence owing to its high accuracy and non-invasiveness. There are several scenarios in measurement practice where this approach cannot be used to conduct measurements while following measurement standards. This study attempted to determine whether measurements performed in such situations were reliable and acceptable. The liquid flow velocity was measured at various distances from the disturbance source, which was the throttle. The measured velocity v_{thr} was compared with the flow velocity in front of the obstruction v_p (reference), which was recorded simultaneously with the required straight sections.

The graphs developed using the measurement results revealed a strong tendency for the velocity to normalize as the distance from the disturbance source (the throttle) increased. As the distance from the throttle increases, the velocity v_{thr} varies less, depending on the angle. The distinctive impact of the throttle on the flow distortion in the settings at the angles of 75° and 90° was also noticeable.

In the measurement section at 1DN, the relative velocity measurement error for the throttle set at a 75° angle reaches almost 12%, and its value varies significantly depending on the angle of the ultrasonic heads. Nonetheless, the angles $\alpha = 180°$ and $\alpha = 300°$, for which the difference in indications upstream and downstream of the throttle is less than 1%, can be found in the 1DN section. The error values δ in the measurement cross-section were far less dependent on the angle of the heads and were less than 7% across the entire range. In the measurement cross-section, apart from the angles of $\alpha = 0°$, $\alpha = 30°$, and $\alpha = 60°$, for which the error values δ surpass 10%, the error values δ for the remaining angles do not exceed 3%.

Changing parameters n, m, and k in the examined velocity distribution equations yielded the best match for the velocity distribution models.

Declaration of Competing Interest

The authors declare that they have no known competing financial interests or personal relationships that could have appeared to influence the work reported in this paper.

Data availability

Data will be made available on request.

References

[1] Q. Mazumder, V.T. Nallamothu, F. Mazumder, Comparison of characteristic particle velocities in solid-liquid multiphase flow in elbow, Int. J. Thermofluids 5 (2020), 100032.
[2] S. AlSaqoor, A. Alahmer, F. Al Quran, A. Andruszkiewicz, K. Kubas, P. Regucki, W. Wędrychowicz, Numerical modeling for the retrofit of the hydraulic cooling subsystems in operating power plant, Therm. Eng. 64 (2017) 551–558.
[3] G. Crewdson, M. Lappa, Thermally-driven flows and turbulence in vibrated liquids, Int. J. Thermofluids 11 (2021), 100102.
[4] D. Zheng, P. Zhang, T. Xu, Study of acoustic transducer protrusion and recess effects on ultrasonic flowmeter measurement by numerical simulation, Flow Meas. Instrum. 22 (2011) 488–493.
[5] R. Raišutis, Investigation of the flow velocity profile in a metering section of an invasive ultrasonic flowmeter, Flow Meas. Instrum. 17 (2006) 201–206.
[6] G. Rajita, N. Mandal, Review on transit time ultrasonic flowmeter, in: 2016 2nd Int. Conf. Control. Instrumentation, Energy Commun., IEEE, 2016: pp. 88–92.
[7] Z. Tang, Research on the key technology of multi-channel gas ultrasonic flowmeter field compensation, Zhejiang University, China, 2015. Ph.D. Thesis.
[8] Y. Sun, T. Zhang, D. Zheng, New analysis scheme of flow-acoustic coupling for gas ultrasonic flowmeter with vortex near the transducer, Sensors. 18 (2018) 1151.
[9] D. Chen, H. Cao, B. Cui, Study on flow field and measurement characteristics of a small-bore ultrasonic gas flow meter, Meas. Control. 54 (2021) 554–564.
[10] L. Qin, L. Hu, K. Mao, W. Chen, X. Fu, Flow profile identification with multipath transducers, Flow Meas. Instrum. 52 (2016) 148–156.
[11] C.V. Palau, G.V. do Bomfim, B.M. de Azevedo, I.B. Peralta, Numerical study of upstream disturbances on the performance of electromagnetic and ultrasonic flowmeters, Sci. Agric. 77 (2020) 1–8.
[12] H. Zhang, C. Guo, J. Lin, Effects of velocity profiles on measuring accuracy of transit-time ultrasonic flowmeter, Appl. Sci. 9 (2019) 1648.
[13] D.V. Mahadeva, R.C. Baker, J. Woodhouse, Further studies of the accuracy of clamp-on transit-time ultrasonic flowmeters for liquids, IEEE Trans. Instrum. Meas. 58 (2009) 1602–1609.
[14] A.S. Awad, Z. Abulghanam, S.M. Fayyad, S. Alsaqoor, A. Alahmer, N. Aljabarin, P. Piechota, A. Andruszkiewicz, W. Wędrychowicz, P. Synowiec, Measuring the Fluid Flow Velocity and Its Uncertainty Using Monte Carlo Method and Ultrasonic Technique, Wseas Trans. Fluid Mech. 15 (2020) 172–182.
[15] P. Synowiec, P. Piechota, W. Wędrychowicz, A. Andruszkiewicz, Analiza dokładności wskazań przepływomierza ultradźwiękowego w pomiarze za kolanem rurociągu, Przegląd Elektrotechniczny. 93 (2017).
[16] P. Piechota, P. Synowiec, W. Wędrychowicz, A. Andruszkiewicz, Ultradźwiękowe pomiary strumieni jednofazowych za kolanem rurociągu, Elektron. Konstr. Technol. Zastos. 58 (2017).
[17] P. Piechota, P. Synowiec, A. Andruszkiewicz, W. Wędrychowicz, Selection of the relevant turbulence model in a CFD simulation of a flow disturbed by hydraulic elbow—comparative analysis of the simulation with measurements results obtained by the ultrasonic flowmeter, J. Therm. Sci. 27 (2018) 413–420.
[18] C.V. Palau, I. Balbastre, J. Manzano, B.M. Azevedo, G.V. Bomfim, Numerical analysis of woltman meter accuracy under flow perturbations, Water. 11 (2019) 2622.
[19] L.A. Salami, Application of a computer to asymmetric flow measurement in circular pipes, Trans. Inst. Meas. Control. 6 (1984) 197–206.
[20] P.I. Moore, G.J. Brown, B.P. Stimpson, Ultrasonic transit-time flowmeters modelled with theoretical velocity profiles: methodology, Meas. Sci. Technol. 11 (2000) 1802.
[21] Y. Pistun, V. Roman, F. Matiko, Investigating the Ultrasonic Flowmeter Error in Conditions of Distorted Flow Using Multipeaks Salami Functions, Metrol. Instrum. (2019) 14–19.
[22] S. Waluś, Mathematical modelling of an ultrasonic flowmeter primary device, Arch. Acoust. 23 (2014) 429–442.
[23] S. Waluś, The possibility of the analytical setting of ultrasonic flow-meter characteristic in the standard conditions of settlement, Zesz. Nauk. Politech. Śląskiej. 969 (1988) 273–282.